ISSN 2347 - 3983
Volume 9. No. 7, July 2021
International Journal of Emerging Trends in Engineering Research
Available Online at http://www.warse.org/IJETER/static/pdf/file/ijeter03972021.pdf
https://doi.org/10.30534/ijeter/2021/03972021

Effect of Oxide Shell on Aluminium Nanoparticle Oxidation Using Molecular Dynamics Simulation

Haidzar Nurdiansyah[1], Boy Arief Fachri [2], Mahros Darsin[3]
[1]Mechanical Engineering Department, University of Jember, Indonesia, haidzarbagus@gmail.com
[2]Mechanical Engineering Department, University of Jember, Indonesia, fachri.teknik@unej.ac.id
[3]Mechanical Engineering Department, University of Jember, Indonesia, mahros.teknik@unej.ac.id

ABSTRACT

Molecular dynamics simulation using reactive force field (ReaxFF) potential was implemented to study the oxidation mechanism in aluminium particles with two different alumina shells. That is, without an oxide shell and with a 1 nm oxide shell. In particular, this research investigated the atomic diffusivity of the system on the oxide shell effect. The results showed that in the heating process, oxygen molecules were adsorbed on the surface of the shell and then diffused to the particle core as the heating temperature increased. The diffusivity of oxygen molecules in the aluminium core which causes the oxidation process to occur, shows that the particles without the oxide shell are faster than the particles with the oxide shell. Although after relaxation, there are similarities in having an oxide shell. However, the thickness is different. This shows that the coating on Al particles can inhibit the rate of oxidation. The thickness of the oxide shell also affects the rate of oxidation.

Key words : Aluminium nanoparticles, molecular dynamics, oxidation mechanism, oxidation rate, reaxFF.

1. INTRODUCTION

Nanotechnology is the study of material science and engineering at the nanometre scale. Nanotechnology has been widely studied in various subjects such as in the fields of materials, military, agriculture, to health [1-4]. Nanoparticles are one of the most important parts of nanotechnology because they have been widely applied in various fields. In general, nanoparticles can be interpreted as a particle with a size of 1-100 nm [5]. Nano-sized materials have different properties from larger size-scale materials such as micrometres [6]. In addition, nanostructured materials have interesting characteristics because they have new potential applications. Aluminium is an easily oxidized material and is widely used in the synthesis of aluminium oxide. Aluminium oxide or alumina is a thin layer formed from the reaction between aluminium and oxygen. Alumina has many uses in electronics, catalysts and thermal fields [7-9]. In the process of alumina synthesis using aluminium oxidation process occurs, where aluminium particles react with oxygen molecules. Studies on the oxidation of aluminium nanoparticles have been carried out by many experimental researchers. Such as nano-aluminium reactivity as measured using transmission electron microscopy (TEM) [10], structure and morphology of aluminium oxide film [11], and oxidation of aluminium at high temperature with various gases [12]. However, experimental explanations of aluminium oxidation have not been able to explain atomic oxidation. Therefore, it is necessary to do research that can explain the atomic oxidation.

There are many simulation methods. However, to analyse at the micro or nano-scale, based on the behaviour of atoms and molecules, the molecular dynamic (MD) simulation method can be used. Even this method can provide extra accuracy compared to other methods such as Finite Element Method (FEM) [13]. Molecular dynamics simulation method is one method that can explain atomic oxidation. LAMPS (Large-scale Atomic/ Molecular Massively Parallel Simulator) is a classical molecular dynamics software which often used in research. The movement of molecules is affected by the potential created by the forces of the surrounding particles. This potential keeps the atom in its position. One of the potential molecular dynamics simulations that are often used in oxidation simulations is the reactive force field function (reaxFF), which was introduced by Van Duin, et al [14]. The reaxFF potential is able to explain the bond-order characteristics in the form of the process of forming and breaking atomic bonds.

Several studies on aluminium oxidation using molecular dynamics simulation methods have been carried out by researchers. Zeng, et al [15] investigated the core-shell oxidation response on aluminium nanoparticles with a size of 4 nm with an oxide shell thickness of 0.5-1 nm using the reaxFF potential. They found that in the 1 nm oxide shell, it melts at 1153 K and the melting point increases as the oxide shell thickness increases. After heating, the corresponding

atomic diffusivity also decreases and particle explosion occurs. Clark et al. [16] also perform molecular dynamics simulations on aluminium particles to determine the oxidation kinetics and identify the oxidation stage when heating. The potential used is the embedded atom method (EAM). The rate of oxygen absorption increases as the heating rate increases. This is caused by the melting of the alumina shell and the ejection of Al atoms to the surrounding Oxygen atoms which causes oxidation. Zhang et al. [17] also investigated the oxidation of aluminium particles caused by oxygen and ethanol. The potential used is reaxFF with canonical ensemble and also micro canonical ensemble to investigate ethanol oxidation. They concluded that oxidation with molecular oxygen was easier than with ethanol. The effect of the presence of an oxide shell on the aluminium oxidation process cannot be ignored. Therefore, we tried to study the use of shells in aluminium oxidation simulations using molecular dynamic simulation methods. To achieve this goal, we used the ReaxFF potential to examine the interactions of aluminium atoms and oxygen atoms from an atomistic scale perspective. This study discusses molecular dynamic simulation with the ReaxFF potential of the oxidation of single Al particles with the difference between the presence and absence of shells, and to understand the growth mechanism of oxide shells.

2. COMPUTATIONAL METHODS

The computational method is carried out using LAMPS software with reaxFF (reactive force field) as a potential. The reaxFF potential is used to describe the bond order and bond energies. Moreover, it is able to accurately describe the dynamic bond formation, dissociation and charge transfer between atoms. The empirical formula for ReaxFF potential can be shown in equation (1).

$$E_{system} = E_{bond} + E_{over} + E_{under} + E_{lp} + E_{val} + E_{tors} + E_{vdWaals} + E_{coulomb} \quad (1)$$

E_{system} showing the total energy of the system, bond energy E_{bond}, over coordination E_{over}, under-coordination E_{under}, lone-pair E_{lp}, valence angle E_{val}, van der Waals $E_{vdWaals}$, dan Coulomb $E_{Coulomb}$ [14].

The Al core used in this simulation has an FCC lattice structure and a particle diameter of 8 nm. The aluminium nanoparticle system is denoted as ANP which consists of two variations, namely aluminium nanoparticles without an oxide shell denoted as nsANP and aluminium with an oxide shell with a thickness of 1 nm denoted as sANP. In sANP, the gap between the core and the shell is 1 Å. During the ANP simulation process, relaxation was carried out for 10 ps and then heated to 3500 K for 500 ps. The heating rate is 10^{13} K/s, then a cooling process is carried out by applying a canonical ensemble (NVT) with a cooling rate of 10^{14}K/s until it reaches a temperature of 300 K.

The dimensions of the box used are 320×320×7 Å with periodic boundaries. Molecular oxygen is distributed randomly with an atomic number of 5455. In this simulation, a canonical ensemble with the Nose/Hoover thermostat method is used [15]. OVITO [18] is used as a post-processing software and visualization tool for simulation results. Figure 1 presents the ANP simulation model. Figure 1a is an aluminium nanoparticle without an oxide shell (nsANP) and Figure 1b is an aluminium nanoparticle with a 1 nm oxide shell (nsANP). The grey colour is the Al atom and the blue is the O atom.

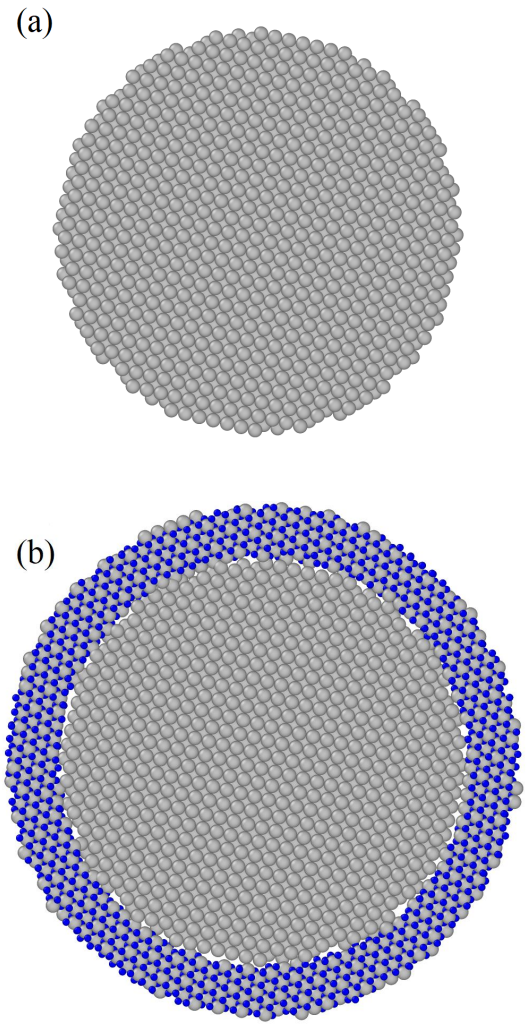

Figure 1: Model simulation ANP (s) nsANP; (b) sANP.

3. RESULTS AND DISCUSSION

The oxidation process in ANP in an oxygen environment can be shown in Figure 2. The red atoms are Al atoms and the blue

atoms are oxygen in the initial system, while the grey atoms are oxygen in the environment. During heating, the surrounding O atoms adhere to the surface of the ANP shown in Figure 2a. As the core begins to melt, the Al atoms in the core start to diffuse into the oxide shell. Then, the molecular Oxygen adsorption continues (see Figure 2b). In Figure 2c, O atoms in the shell and O atoms in the environment diffuse to the particle core sequentially. This shows the core oxidation process takes place. In sANP, O atoms in the environment continue to diffuse into the core, and the shell does not break. This result is in line with the finding of Zhang et al. [18]. Whereas, in nsANP, after the shell has been formed, it maintains its position. As the temperature increases, the shell then breaks.

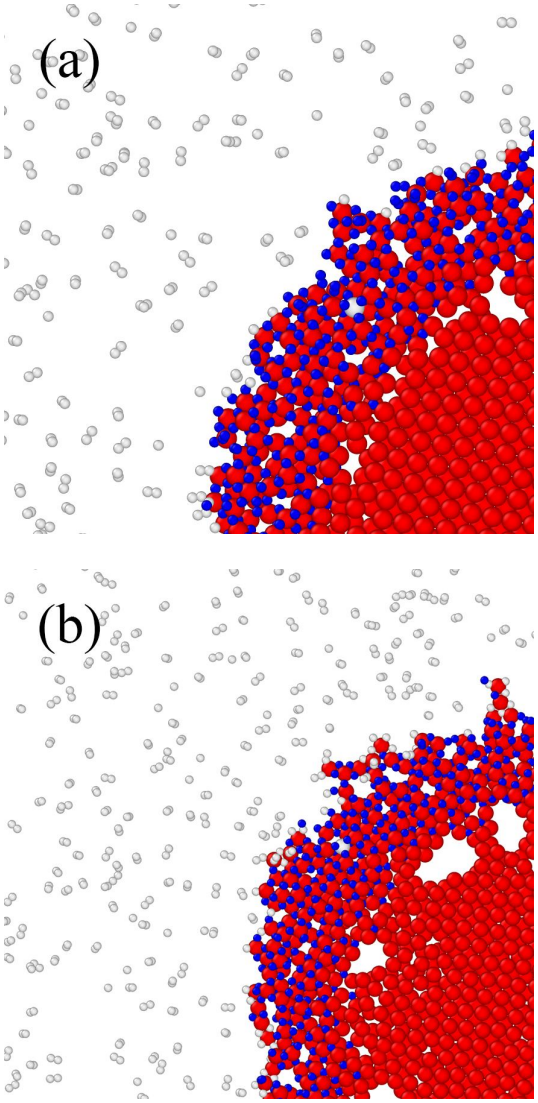

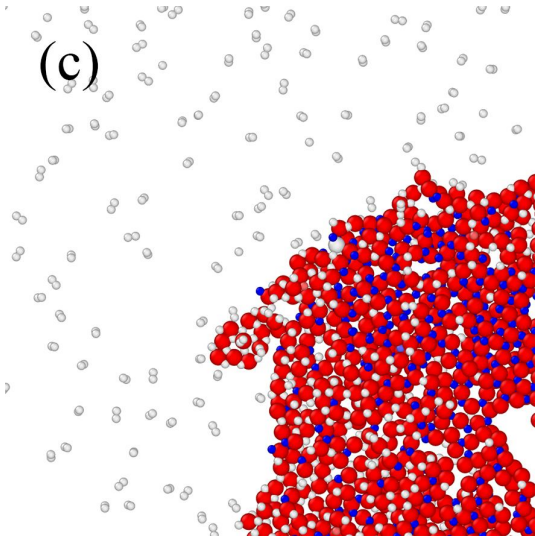

Figure 2: Snapshot of oxidation mechanism in sANP; (a) 100 ps; (b) 300 ps (c) 500 ps.

Figure 3 represents the level of oxidation in ANP. In nsANP, the oxidation state increases slowly from 0 ps to 200 ps. Then, the oxidation state increased sharply and oxidized overall at 400 ps. While in sANP, the increase in oxidation level was seen slowly from 0 ps to 300 ps. Then it rose significantly at 400 ps. In sANP, it is completely oxidized at 600 ps. This shows that the presence of an oxide shell on aluminium nanoparticles can inhibit the rate of oxidation. Although nsANP formed an oxide shell during the relaxation process, the thickness of the oxide was different from that of sANP. This is in line with Zeng et al. [15] that the oxide shell affects the oxidation process on aluminium nanoparticles.

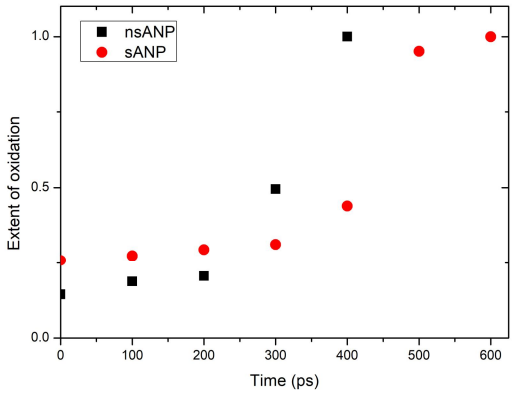

Figure 3: Extent of oxidation on ANP.

Figure 4 shows a graph of potential energy against temperature. At the initial stage of heating, the graph of the potential energy of nsANP shown in Figure 4a slowly decreases followed by slow oxidation to a temperature of about 2000 K at 266 ps. Then, the graph decreased drastically to a temperature of 2850 K at 400 ps, which indicated that all of the Al atoms were bonded to O atoms. Meanwhile, in sANP, the graph of potential energy was shown in Figure 4b.

The potential energy graph slowly decreases as the temperature increases to a temperature of about 2700 K. At this stage, it is marked by the adsorption of oxygen molecules from the environment to the shell surface. Then there was a significant decrease to a temperature of 3500 K and continued with a cooling temperature of up to 3000 K. An increase in oxidation occurred at 400 ps and significantly up to 600 ps. In the heating to cooling stage, ANP undergoes an expansion process until the shell breaks in nsANP and is followed by a contraction process. The expansion of the particles is due to the initial gap between the core and the oxide shell [19].

The radial distribution function (RDF) of the Al-O bond at 400 ps can be shown in Figure 5a. The initial peak appears at 1.875 Å and increases until it becomes sharper at a later stage. The RDF peak of the Al-O nsANP bond at 400 ps indicates the coordination number of 19.6. Meanwhile, the peak of RDF of Al-O sANP at 400 ps showed that the coordination number of 8.3 was lower than that of nsANP. Figure 5b is the Al-Al bond RDF peak.

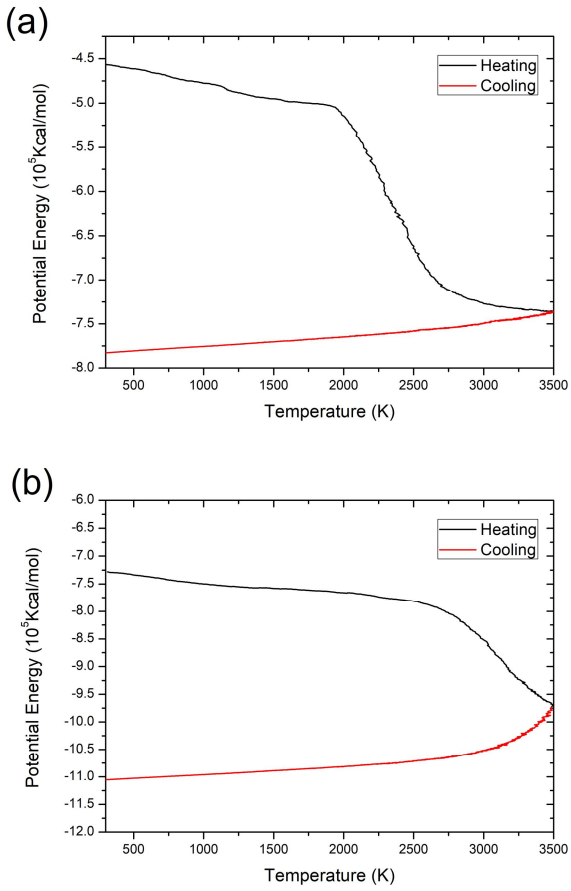

Figure 4: Graph of potential energy against temperature; (a) nsANP; (b) sANP.

The initial peak appears at 2.775 Å, at 400 ps the Al-Al bond RDF coordination number for nsANP is 42.36. While the coordination number in sANP is 22.43. Figure 5c shows the RDF peak of the O-O bond. The nsANP and sANP peaks appeared at 1.275 Å. The nsANP coordination number at 400 ps shows at 14.28. In the RDF coordination number, the O-O bond in sANP shows at 13.32 which is lower than nsANP.

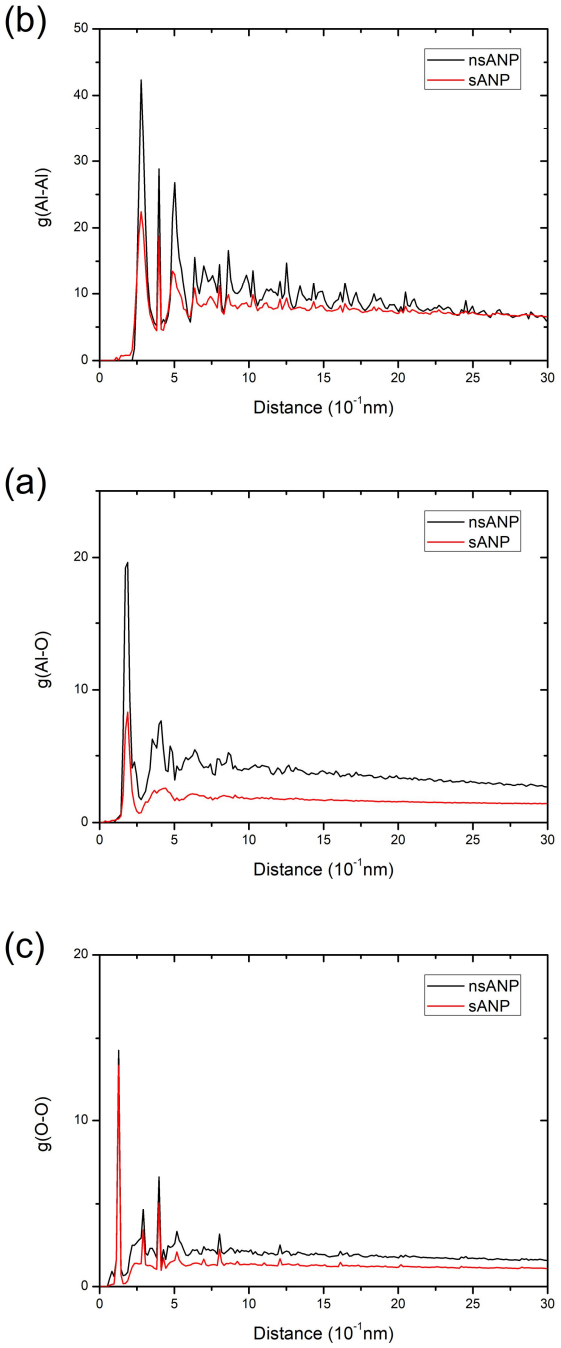

Figure 5: Radial distribution function at 400 ps (a) RDF of Al-O bond; (b) RDF of Al-Al bond; (c) RDF of O-O bond.

In nsANP, the Al/O ratio shows at 1:1.87, while in sANP, the Al/O ratio is 1:1.29. This indicates that at 400 ps, sANPs are less O atoms than nsANPs. When viewed from the charge distribution at 400 ps as shown in Figure 6, the average Al charge value in sANP (0.64), which is lower than that of nsANP (1.03). While, the average value of O charge on

nsANP is -0.5 and -0.53 on sANP. Different charge densities on the ANP surface can cause significantly different surface reactivity [20].

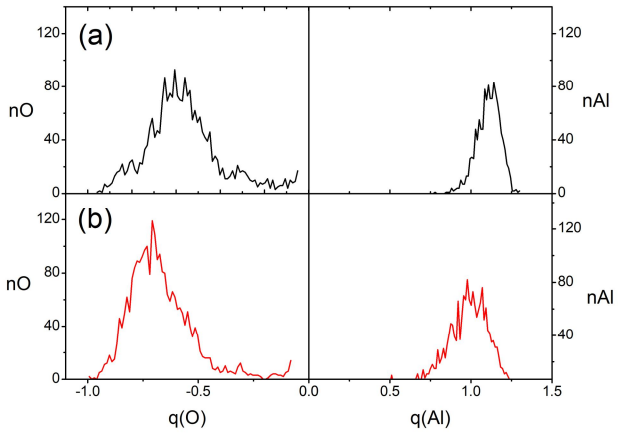

Figure 5: Charge distribution; (a) nsANP; (b) sNAP.

4. CONCLUSION

In this study, we simulated the molecular dynamics method with ReaxFF potential and canonical ensemble (NVT) on 8 nm aluminium particles with the difference between no alumina shell and 1 nm alumina shell. The results showed that, during the heating process, oxygen molecules began to be adsorbed and then diffused towards the particle core as the heating temperature increased. The diffusivity of oxygen molecules in the aluminium core, which causes the oxidation process to occur, shows that nsANP is faster than sANP. Although after relaxation there are similarities in oxide shells but have different thicknesses. This shows that shelling Al particles can inhibit the rate of oxidation. The thickness of the oxide shell also affects the rate of oxidation.

ACKNOWLEDGEMENT

We are grateful for the support from the Applied Technology Laboratory, Faculty of Engineering, University of Jember, which has facilitated running the simulation in this research.

REFERENCES

1. M.N. Shalaby and M.M. Saad, **Advanced Material Engineering and Nanotechnology for Improving Sports Performance and Equipment.** *International Journal of Psychosocial Rehabilitation*, vol. 24, pp. 2314-2322, May 2020.
2. A. Molestina, K. Ravichandran, and M. Welleck, **Military Applications of Nanotechnology.** *Student Papers in Public Policy*, vol. 2, pp. 5, April 2020.
3. M. Usman, M. Farooq, A. Wakeel, A. Nawaz, S.A. Cheema, H.u. Rehman, I. Ashraf, and M. Sanaullah, **Nanotechnology in agriculture: Current status, challenges and future opportunities.** *Science of The Total Environment*, vol. 721, pp. 137778, June 2020.
4. G. Perry, F. Cortezon-Tamarit, and S.I. Pascu, **Detection and monitoring prostate specific antigen using nanotechnology approaches to biosensing.** *Frontiers of Chemical Science and Engineering*, vol. 14, pp. 4-18, Feb. 2020.
5. L. Calzolai, D. Gilliland, and F. Rossi, **Measuring nanoparticles size distribution in food and consumer products: a review.** *Food Addit Contam Part A Chem Anal Control Expo Risk Assess*, vol. 29, pp. 1183-1193, August 2012.
6. A.B. Morgan, J.D. Wolf, E.A. Guliants, K.A.S. Fernando, and W.K. Lewis, **Heat release measurements on micron and nano-scale aluminum powders.** *Thermochimica acta*, vol. 488, pp. 1-9, May 2009.
7. A. Mozalev, M. Sakairi, H. Takahashi, H. Habazaki, and J. Hubálek, **Nanostructured anodic-alumina-based dielectrics for high-frequency integral capacitors.** *Thin Solid Films*, vol. 550, pp. 486-494, Jan. 2014.
8. K.Y. Paranjpe, **Alpha, Beta and Gamma Alumina as a catalyst -A Review.** *The Pharma Innovation Journal*, vol. 6, pp. 236-238, Nov. 2017.
9. W. Zou, X. Wang, Y. Wu, L. Zou, G.q. Zu, D. Chen, and J. Shen, **Opacifier embedded and fiber reinforced alumina-based aerogel composites for ultra-high temperature thermal insulation.** *Ceramics International*, vol. 45, pp. 644-650, Jan. 2019.
10. A. Rai, K. Park, L. Zhou, and M.R. Zachariah, **Understanding the mechanism of aluminium nanoparticle oxidation.** vol. 10, pp. 843-859, May 2006.
11. L.P.H. Jeurgens, W.GSloof, F.DTichelaar, and E.J. Mittemeijer, **Structure and morphology of aluminium-oxide films formed by thermal oxidation of aluminium.** *Thin Solid Films*, vol. 418, pp. 89-101, Oct. 2002.
12. R.J. Breakspere, **High□temperature oxidation of aluminium in various gases.** *Journal of Applied Chemistry*, vol. 20, pp. 208-212, July 1970.
13. S. Nirwal and R. Katukam, **An approach for Coupling FEM & Molecular Dynamics.** *International Journal of Emerging Trends in Engineering Research (IJETER)*, vol. 3, pp. 07 – 19, Oct. 2015.
14. A.C.T.v. Duin, S. Dasgupta, F. Lorant, and W.A. Goddard, **ReaxFF: A Reactive Force Field for Hydrocarbons.** *The Journal of Physical Chemistry A*, vol. 105, pp. 9396-9409, Oct. 2001.
15. H. Zeng, X. Cheng, C. Zhang, and Z. Lu, **Responses of Core–Shell Al/Al2O3 Nanoparticles to Heating: ReaxFF Molecular Dynamics Simulations.** *The Journal of Physical Chemistry C*, vol. 122, pp. 9191-9197, 2018/04/26 2018.
16. R. Clark, W. Wang, K.-i. Nomura, R. Kalia, A. Nakano, and P. Vashishta, **Heat-Initiated Oxidation of an Aluminum Nanoparticle.** *MRS Proceedings*, vol. 1405, pp. December 2012.

17. Y. RanZhang, A.C.T.v. Duin, and K.H. Luo, **Investigation of ethanol oxidation over aluminum nanoparticle using ReaxFF molecular dynamics simulation.** *Fuel*, vol. 234, pp. 94-100, Dec. 2018.
18. Q. Chu, B. Shi, L. Liao, K.H. Luo, N. Wang, and C. Huang, **Ignition and Oxidation of Core–Shell Al/Al2O3 Nanoparticles in an Oxygen Atmosphere: Insights from Molecular Dynamics Simulation.** *The Journal of Physical Chemistry C*, vol. 122, pp. 29620-29627, 2018/12/27 2018.
19. Y.-T. Zheng, M. He, G.-x. Cheng, Z. Zhang, F.-Z. Xuan, and Z. Wang, **Effect of ionizationn on the oxidation kinetics of aluminum nanoparticles.** *Chemical Physics Letter*, vol. 696, pp. 8-11, 2018.
20. S. Alavi, J.W. Mintmire, and D.L. Thompson, **Molecular Dynamics Simulations of the Oxidation of Aluminum Nanoparticles.** *The Journal of Physical Chemistry B*, vol. 109, pp. 209-214, Jan. 2005.